Direct spectroscopy of a deep two-dimensional photonic crystal microresonator

P. Kramper,[1] A. Birner,[2,*] M. Agio,[3,4] C. M. Soukoulis,[4,5] F. Müller,[2] U. Gösele,[2] J. Mlynek,[1,†] and V. Sandoghdar[1,‡]
[1]*Fachbereich Physik, Universität Konstanz, 78457 Konstanz, Germany*
[2]*Max-Planck-Institut für Mikrostrukturphysik, Weinberg 2, 06120 Halle, Germany*
[3]*INFM, Dipartimento di Fisica "A. Volta," Università di Pavia, 27100 Pavia, Italy*
[4]*Ames Laboratory, Iowa State University, Ames, Iowa 50011*
[5]*Research Center of Crete, Heraklion, Crete, Greece*
(Received 13 June 2001; published 8 November 2001)

Photonic crystals based on macroporous silicon with fundamental band gaps in the middle infrared region 3.4–5.8 μm were fabricated. Scanning probe optical microscopy and laser spectroscopy were combined to examine a *deep* two-dimensional photonic crystal microresonator based on a single point defect. Two sharp resonances were recorded in the band gap, in excellent agreement with the results of numerical simulations. Such a microresonator with high-quality factors and a subwavelength mode extension could be used for a range of applications including integrated optical gas sensors.

DOI: 10.1103/PhysRevB.64.233102 PACS number(s): 42.70.Qs, 42.50.−p, 42.62.−b, 42.82.−m

Since the pioneering proposals by Yablonovitch[1] and John[2] in 1987 photonic crystals have received considerable attention from a wide scientific community.[3] Being the three-dimensional analog of a Bragg reflector, a photonic crystal can possess frequency band gaps within which propagation of light is inhibited for all polarizations and directions. A single point defect in the crystal, however, can suffice to give rise to isolated sharp resonances in the gap spectrum and to spatial confinement of the electromagnetic field around the defect.[4] The expected high quality factors (Q) and the possibility of custom designing light propagation make such photonic crystal microresonators promising candidates for a range of novel and efficient optical devices.[5,6]

The demonstration of photonic crystal micro-resonators has advanced most rapidly for one- and two-dimensional photonic crystals due to the availability of well-established methods such as high resolution lithography and etching techniques. Nevertheless, realization of high-quality photonic crystals with depth of numerous wavelengths remains a nontrivial problem. As a result, recent efforts have concentrated on very thin photonic crystals[7–11] surrounded by media of lower dielectric constants where propagation relies partly on index guiding. In this paper we present measurements of sharp resonances in a *deep* two-dimensional photonic crystal microresonator. Such a photonic crystal is of fundamental interest because it acts as a true two-dimensional system in which the only mechanism for controlling light propagation is based on photonic band gaps.

Two-dimensional photonic crystals fabricated by electrochemical preparation of macroporous silicon[12] have been shown to contain wide full band gaps centered in the spectral region between 20 μm and 1.3 μm.[13–16] Figure 1(a) shows the top view of such a crystal used in our experiment, consisting of an array of air cylinders with a lattice constant of $a=1.5$ μm and depth of 100 μm, into which two line defects and an isolated point defect have been incorporated. The central part of the sample around the point defect acts as a two-dimensional optical cavity, and the two line defects serve as waveguides for coupling in and out of this resonator. As displayed in Fig. 1(b), the sample has been micromachined by isotropic plasma etching[17] in order to arrive at a barlike structure convenient for handling and performing optical measurements. The solid curve in Fig. 1(c) shows the transmission spectrum of the structure obtained from Fourier transform infrared spectroscopy (FTIR) with the TE-polarized light. We note that no resonance in the band gap was detected; this is due to the fact that FTIR is based on white light illumination of a large area and is therefore in-

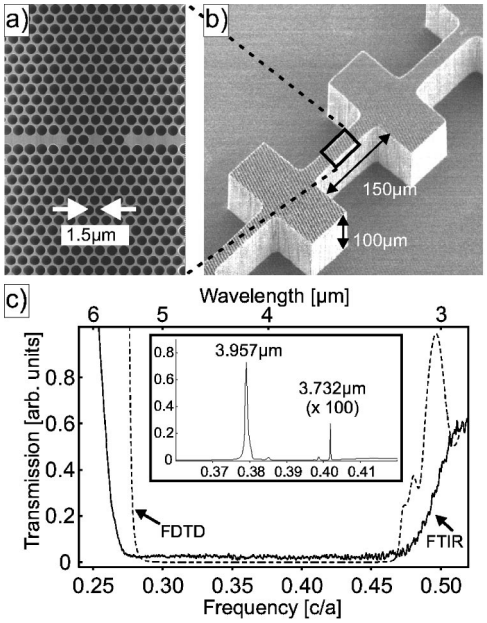

FIG. 1. (a) A top view of a zoom into the region of the crystal containing the microresonator. (b) An overview of the photonic crystal substrate. (c) The solid curve shows the band gap spectrum of the structure in (b) measured by FTIR; the sensitivity of this method is inadequate for detecting the influence of the defects. The dashed curve displays the outcome of numerical simulations (FDTD) for a crystal without defects. When defects are introduced two resonances appear, as shown in the insert. The horizontal axis is in reduced units of c/a where c is the speed of light and a is the lattice constant. The corresponding values of the wavelength in our experiment are indicated on the upper horizontal axis.

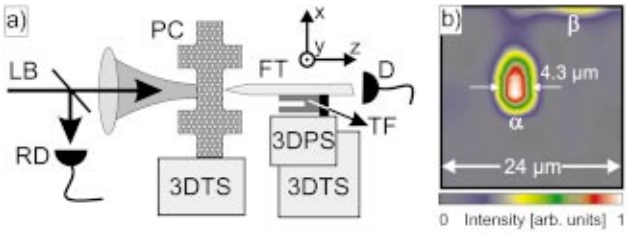

FIG. 2. (Color) (a) Schematics of the setup for the optical measurements. The laser beam (LB) is focused onto the first waveguide at the entrance facet of the photonic crystal (PC). The transmitted light is collected locally with an uncoated optical fiber tip (FT) at the exit of the second waveguide. RD, 3DTS, 3DPS, TF, and D stand for reference detector, three-dimensional translation stage, three-dimensional piezo-scanner, quartz tuning fork and detector, respectively. (b) A typical raster-scanned image obtained at the output facet of the crystal in the xy plane, represented by a linear color scale.

sensitive to local defects. The band edges at 3.4 μm and 5.8 μm, however, are clearly observed and well reproduced by two-dimensional finite difference time domain (FDTD) calculations for the structure without any defects [see the dashed curve in Fig. 1(c)]. By optimizing the agreement between the numerical and experimental band edge frequencies, we deduced the pore diameter to be $2r=1.31$ μm and then repeated the FDTD simulations taking into account the defects [see Fig. 1(a)]. As displayed in the insert of Fig. 1(c), two sharp resonances were obtained within the fundamental band gap at nominal wavelengths of 3.732 μm and 3.957 μm. Below we discuss the experimental investigation of these.

Some of the recent activities have successfully used internal light sources such as semiconductor emitters embedded in the structure[18,19] to perform spectroscopy on photonic crystal microresonators, but for studies in the middle infrared region this is not an option. External excitation of high-Q modes spatially bound to a region of subwavelength dimensions, on the other hand, requires a widely tunable and intense laser source with a narrow linewidth and good beam quality. We have used a continuous-wave optical parametric oscillator (OPO) with a linewidth of about 100 kHz, tunable

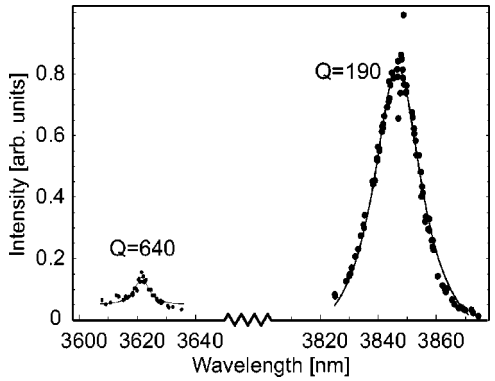

FIG. 3. Two of high-Q resonances centered at wavelengths 3.621 and 3.843 μm. The Lorentzian profiles were fitted to the experimental data and yield quality factors of 640 and 190.

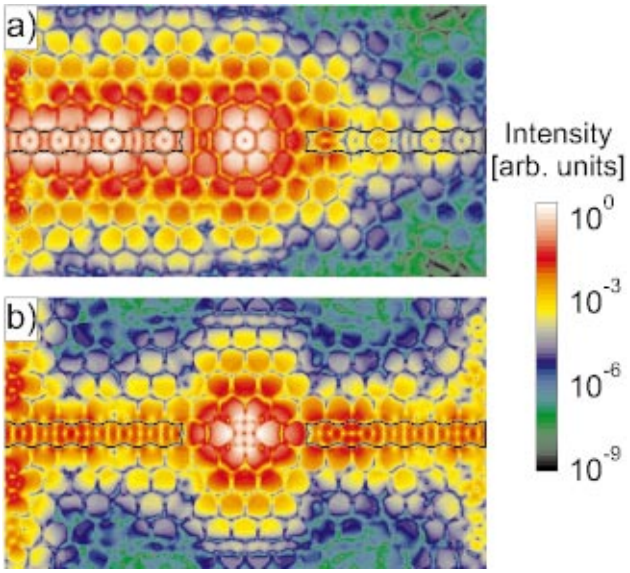

FIG. 4. (Color) Spatial intensity distribution of the optical intensity in the photonic crystal for (a) the mode at $\lambda=3.621$ μm and (b) the mode at $\lambda=3.843$ μm. The contours of the two line defects are marked by black lines for clarity.

in the range of 1.4–1.55 μm and 3.6–4 μm and a nearly TEM_{00} Gauss mode.[20] The laser beam is focused to a spot with a full-width at half-maximum (FWHM) of about 6 μm using a sapphire lens with a focal length of 25 mm [see Fig. 2(a)]. The intensity of the incident laser beam is modulated at 2 kHz by a mechanical chopper to allow lock-in detection. A reference detector is used to monitor the incident laser power, allowing to make corrections due to the variation of intensity at different wavelengths. A fine rotation stage and a three-dimensional translation stage are used to place the entrance plane of the photonic crystal in the laser focus. An uncoated tapered fluoride glass fiber with a core of 9 μm suitable for monomode guiding in the middle-infrared regime is mounted in a scanning near-field optical microscope (SNOM) head and is used as a local detector. A three-dimensional translation stage and a three-dimensional piezo scanner allow precise positioning and scanning of the fiber tip against the exit facet of the photonic crystal while being monitored under an optical microscope. A quartz tuning fork is used to monitor or to control the distance between the tip end and the sample surface via the shear force signal common in SNOM.[21] The light exiting the far end of the fiber probe is detected using a PbSe photoconductive detector after passing through a long-pass filter that only transmits light of wavelength greater than 1.8 μm.

Figure 2(b) displays a raster-scanned image of the optical intensity distribution at the wavelength of 3.84 μm as recorded by the fiber probe at the crystal exit in the xy plane [see also Fig. 2(a)]. The elongated bright spot labeled α in the middle indicates the light that exits the second waveguide. Given the waveguide width of about 1.5 μm and the observed FWHM of 4.3 μm, we estimate the lateral spatial resolution to be of the order of one wavelength. The vertical extent of this spot is about 6.5 μm, in very good agreement with our independent measurements of the focus spot in the

incident laser beam. This is a clear demonstration that although there is no confinement in the third dimension, the laser beam remains intact while traversing the photonic crystal. A second weak spot labeled β in the upper part of the image 2(b) indicates the tail of the stray light that arrives at the exit plane by traveling over the photonic crystal. The assignments of α to the light exiting the microresonator and β to the stray light could be verified by studying the dependence of the light intensity as a function of tip-sample distance z. As the tip was retracted, the intensity in α dropped rapidly over a distance of about 10 μm and the spot became round, whereas neither the intensity nor the shape of β changed. This confirms that the light in α originates from a confined region of the waveguide and is therefore highly divergent whereas the light in β, being a part of a freely propagating field, has a much lower divergence. The image in Fig. 2(b) nicely demonstrates the advantage of a local detector for investigating micro-resonators where the coupling of free beams is often accompanied by a considerable background stray light.

We have recorded a series of images such as that in Fig. 2(b) for laser wavelengths between 3.6 μm and 3.9 μm. By plotting the maximum power values in the spot α we have been able to map directly two resonance profiles centered at 3.621 μm and 3.843 μm, shown in Fig. 3. The spot α vanished completely for off-resonant wavelengths. The positions of the measured resonance frequencies differ slightly from those predicted in the insert of Fig. 1(c) but agree extremely well with the calculated values of 3.625 μm and 3.834 μm if one allows for the pores neighboring the defects to be about 4.3% wider than the bulk value of 1.31 μm. As has been pointed out previously,[22] this small deviation is due to a slightly different dynamics of the pore formation close to defects.

Having obtained a very good agreement between theory and experiment for two resonance frequencies, we can now rely on the FDTD calculations to attribute these resonances to certain spatial modes. Figures 4(a) and 4(b) show the intensity distributions for the two resonances centered at 3.621 μm and 3.843 μm, respectively. Although in both cases the electromagnetic energy is highly confined to an area of $A \sim 0.9\lambda^2$, its spatial character varies substantially. A proper knowledge of the spatial modes is particularly important for controlling and determining the coupling of the microresonator with an active medium. In future work we plan to apply SNOM to the crystal-air interface in order to visualize the intensity distribution around the defects directly.[23]

One of the biggest challenges in microcavity conception is to maximize the quality factor Q while reducing the size of the cavity because the latter typically leads to diffraction or scattering and therefore to a reduction in Q. In a one-dimensional Fabry-Perot resonator the success of this combination is summarized by the so-called cavity finesse $\mathcal{F} = c/2n_{\mathrm{med}}L\Delta\nu$, where $\Delta\nu$, L, and n_{med} indicate the resonance linewidth, the cavity length, and the medium index of refraction, respectively.[24] Our resonator is two-dimensional while other demonstrations of micro-resonators have used three-dimensional confinement of light to achieve high-quality factors. For example, for GaAs microdisks $Q \sim 12000$ and $V \sim 6\lambda_{\mathrm{med}}^3$ have been obtained while for GaAs/AlAs micropillars the Q has been reported to reach 2100 in a cavity with $V \sim 5\lambda_{\mathrm{med}}^3$.[25] In order to have a common measure for comparison of various cavities, we propose to extend the concept of $\mathcal{F}$ to higher dimensions by using $\mathcal{F} = Q/\rho(\lambda)$ with $\rho(\lambda) = dN/(d\lambda/\lambda)$ denoting the dimensionless density of modes. This definition yields $\mathcal{F}_{2D} = \lambda_{\mathrm{med}}^2 Q/2\pi A$ and $\mathcal{F}_{3D} = \lambda_{\mathrm{med}}^3 Q/4\pi V$ where A and V indicate the mode area and volume, and λ_{med} is the wavelength in the medium. By fitting Lorentzian profiles to the resonances in Fig. 3 we obtain quality factors of 640 and 190. Although these Q values are not very high, the extremely small mode areas in our photonic crystal resonator result in generalized finesse $\mathcal{F}_{2D}$ of 115 and 34 for the two resonances, comparable with $\mathcal{F}_{3D} \sim 150$ for the microdisk and $\mathcal{F}_{3D} \sim 33$ for the micropillars. Such high finesse have also been achieved in photonic crystal slabs where the mode volume can reach the order of λ_{med}^3.[26]

For a photonic crystal microcavity Q depends strongly on the number of pores surrounding the defect and on the geometrical considerations such as the filling factor $f = r/a$. The microcavity studied here is separated from two waveguides only by two pores on each side, and the lattice has a very high air filling factor of 0.43, leading to theoretical quality factors of 1950 and 545 as found by numerical simulations for the two modes at $\lambda = 3.621$ μm and 3.843 μm, respectively. The discrepancy between the theoretical and measured values of Q could be due to different effects. First, because a small deviation of about 0.1% in the pore diameters leads to a wavelength shift of about 2.6 nm, any inhomogeneity along the structure depth could broaden the resonance lines. Second, losses due to diffraction or scattering out of the plane of periodicity,[27] as well as possible coupling between the TE and TM modes,[10] have not been accounted for in the theory since our FDTD calculations have been done in two dimensions. Indeed, in order to minimize out-of-plane scattering in thin two-dimensional photonic crystals, low filling factors are needed[8,19] with the compromise of having no full band gap for the TM polarization. In our case due to the extended nature of the structure, we expect out-of-plane losses to play a much less important role. This assumption is supported by the fact that the higher Q belongs to the mode at the shorter wavelength whereas the contrary would have been expected if the Q had been dominated by out-of-plane scattering.[28] We are currently performing three-dimensional FDTD calculations to study these issues in detail.

Although the main focus of our current work has been on spectroscopy, it is of practical interest to address the issue of structure transmissivity. The intrinsic transmissivity of the structure in this work depends on the overlap between the modes of the resonator and the two waveguides. The rotational symmetry of the mode at $\lambda = 3.621$ μm [see Fig. 4(a)], for example, is responsible for a lower coupling efficiency to the waveguides and a higher quality factor whereas the transmission of the mode at $\lambda = 3.843$ μm [see Fig. 4(b)] is expected to be higher, at the cost of a lower Q.[29,30] The direct way to measure the structure transmissivity would be to consider the ratio of the laser power incident on the crystal to that exiting it, but for several reasons this is not an

easy task. First, the efficiency of coupling a focused Gaussian beam to a photonic crystal waveguide of subwavelength width is difficult to estimate due to the nontrivial spatial overlap and due to a high reflectivity at the air-crystal interface. The latter is in turn complicated by the fact that the effective index of refraction of the waveguide is dictated by its dispersion relation.[31] Another unknown factor is the collection efficiency of the optical fiber tip in our arrangement. A quantitative analysis of the transmission is left, therefore, to future work where we plan to follow directly the flow of the electromagnetic energy by applying a near-field probe to the interface between the photonic crystal and air.

In conclusion, we have performed spectroscopy on a deep two-dimensional microresonator in which the propagation of light is only determined by its photonic band structure. Direct application of laser spectroscopy with a widely tunable source and local detection of the transmitted light have made it possible to detect two high-Q resonances and to identify them with distinct spatial modes of the cavity. The recorded generalized finesse of about 115 shows that despite lack of confinement in the third dimension, deep two-dimensional photonic crystals can combine high quality factors with tight confinement of the electromagnetic field to a subwavelength region. The integration of such high-finesse resonators on a microchip also containing laser sources and detectors for absorption spectroscopy of different gases may offer an alternative to the existing optical sensors which use conventional cells or Fabry-Perot resonators.[32] In particular, the deep nature of our structures is expected to be advantageous because it allows probing a large volume of material.

We are grateful to V. Lehmann, S. Ottow, H. Föll, U. Grüning, P. Villeneuve, E. Lidorikis, and R. B. Wehrspohn for many fruitful discussions. We thank S. Schiller for the generous loan of an OPO system in the initial phase of the experiment and M. Beck for help with the data acquisition software. This work was supported by the Deutsche Forschungsgemeinschaft (DFG), Optik-Zentrum Konstanz (OZK), U.S. Department of Energy, and IST project PCIC.

*Present address: Infineon Technologies, Königsbrückerstraße 94, 01099 Dresden, Germany.

†Present address: President, Humboldt Universität zu Berlin, 10099 Berlin, Germany.

‡Author to whom correspondence should be addressed Present address: Laboratorium für Physikalische Chemie, ETH, CH-8093, Zürich, Switzerland. Electronic address: vahid.sandoghdar@ethz.ch

[1] E. Yablonovitch, Phys. Rev. Lett. **58**, 2059 (1987).

[2] S. John, Phys. Rev. Lett. **58**, 2486 (1987).

[3] For an overview see articles in *Photonic Band Gap Materials*, edited by C. M. Soukoulis (Kluwer, Dordrecht, 1996).

[4] J. D. Joannopoulos, R. D. Meade, and J. N. Winn, *Photonic Crystals* (Princeton University Press, Princeton, NJ, 1995).

[5] S. Fan, P.R. Villeneuve, J.D. Joannopoulos, and H.A. Haus, Phys. Rev. Lett. **80**, 960 (1998).

[6] S.G. Johnson, C. Manolatou, S. Fan, P.R. Villeneuve, J.D. Joannopoulos, and H.A. Haus, Opt. Lett. **23**, 1855 (1998).

[7] J.S. Foresi, P.R. Villeneuve, J. Ferrara, E.R. Thoen, G. Steinmeyer, S. Fan, J.D. Joannopoulos, L.C. Kimerling, H.I. Smith, and E.P. Ippen, Nature (London) **390**, 143 (1997).

[8] O. Painter, R.K. Lee, A. Scherer, A. Yariv, J.D. O'Brien, P.D. Dapkus, and I. Kim, Science **284**, 1819 (1999).

[9] T.F. Krauss, R.M. De La Rue, S. Brand, Nature (London) **383**, 699 (1996).

[10] E. Chow, S.Y. Lin, S.G. Johnson, P.R. Villeneuve, J.D. Joannopoulos, J.R. Wendt, G.A. Vawter, W. Zubrzycki, H. Hou, and A. Alleman, Nature (London) **407**, 983 (2000).

[11] N. Kawai, K. Inoue, N. Carlsson, N. Ikeda, Y. Sugimoto, K. Asakawa, and T. Takemori, Phys. Rev. Lett. **86**, 2289 (2001).

[12] V. Lehmann, J. Electrochem. Soc. **140**, 2836 (1993).

[13] U. Grüning, V. Lehmann, and C.M. Engelhardt, Appl. Phys. Lett. **66**, 3254 (1995).

[14] A. Birner, U. Grüning, S. Ottow, A. Schneider, F. Müller, V. Lehmann, H. Föll, and U. Gösele, Phys. Status Solidi B **165**, 111 (1998).

[15] S. Rowson, A. Chelnokonv, and J.-M. Lourtioz, J. Lightwave Technol. **17**, 1989 (1999).

[16] J. Schilling, A. Birner, F. Müller, R.B. Wehrspohn, R. Hillebrand, U. Gösele, K. Busch, S. John, S.W. Leonard, and H.M. van Driel, Opt. Mater. **17**, 7 (2001).

[17] S. Ottow, V. Lehmann, and H. Föll, J. Electrochem. Soc. **143**, 385 (1996).

[18] A. Scherer, O. Painter, B. D'Urso, R. Lee, and A. Yariv, J. Vac. Sci. Technol. B **16**, 3906 (1998).

[19] H. Benisty, C. Weisbuch, D. Labilloy, M. Rattier, C.J.M. Smith, T. F. Krauss, and R.M. De La Rue, J. Lightwave Technol. **17**, 2063 (1999).

[20] K. Schneider, P. Kramper, S. Schiller, and J. Mlynek, Opt. Lett. **22**, 1293 (1997).

[21] K. Karrai and R.D. Grober, Appl. Phys. Lett. **66**, 1842 (1995).

[22] F. Müller, A. Birner, U. Gösele, V. Lehmann, S. Ottow, and H. Föhl, J. Porous Mater. **7**, 201 (2000).

[23] S. Fan, I. Appelbaum, and J.D. Joannopoulos, Appl. Phys. Lett. **75**, 3461 (1999).

[24] B.E.A. Saleh and M.C. Teich, *Fundamentals of Photonics* (Wiley-Interscience, New York, 1991).

[25] J.M. Gérard and B. Gayral, Physical E **9**, 131 (2001).

[26] O. Painter, A. Husain, A. Scherer, J.D. O'Brien, I. Kim, and P.D. Dapkus, J. Lightwave Technol. **17**, 2082 (1999).

[27] B. D'Urso, O. Painter, J. O'Brien, T. Tombrello, A. Yariv, and A. Scherer, J. Opt. Soc. Am. B **15**, 1155 (1998).

[28] P. Pottier, C. Seassal, X. Letartre, J.L. Leclercq, P. Viktorovitch, D. Cassagne, and C. Jouanin, J. Lightwave Technol. **17**, 2058 (1999).

[29] P. Villeneuve, S. Fan, and J.D. Joannopoulos, Phys. Rev. B **54**, 7837 (1996).

[30] M. Agio, E. Lidorikis, and C. Soukoulis, J. Opt. Soc. Am. B **17**, 2037 (2000).

[31] S.W. Leonard, H.M. van Driel, A. Birner, U. Gösele, and P.R. Villeneuve, Opt. Lett. **25**, 1550 (2000).

[32] M. Saito, M. Takizawa, K. Ikegawa, and H. Takami, J. Appl. Phys. **63**, 269 (1988).